IEEE Access
Multidisciplinary ⋮ Rapid Review ⋮ Open Access Journal

Received July 30, 2021, accepted August 23, 2021, date of publication August 27, 2021, date of current version September 7, 2021.

Digital Object Identifier 10.1109/ACCESS.2021.3108406

An Artificial Neural Network System for Photon-Based Active Interrogation Applications

ABBAS J. JINIA[1], (Member, IEEE), TESSA E. MAURER[1], CHRISTOPHER A. MEERT[1], MICHAEL Y. HUA[1], (Member, IEEE), S. D. CLARKE[1], (Member, IEEE), HUN-SEOK KIM[2], (Member, IEEE), DAVID D. WENTZLOFF[2], (Senior Member, IEEE), AND SARA A. POZZI[1,3], (Fellow, IEEE)

[1]Department of Nuclear Engineering and Radiological Sciences, University of Michigan, Ann Arbor, MI 48109, USA
[2]Department of Electrical Engineering and Computer Science, University of Michigan, Ann Arbor, MI 48109, USA
[3]Department of Physics, University of Michigan, Ann Arbor, MI 48109, USA

Corresponding author: Abbas J. Jinia (ajinia@umich.edu)

This work was supported by the U.S. Department of Homeland Security, Countering Weapons of Mass Destruction Office, Academic Research Initiative, under Grant 2016-DN-077-ARI106.

ABSTRACT Active interrogation (AI) is a promising technique to detect shielded special nuclear materials (SNMs). At the University of Michigan, we are developing a photon-based AI system that uses bremsstrahlung radiation from an electron linear accelerator (linac) as an ionizing source and trans-stilbene organic scintillating detectors for neutron detection. Stilbene scintillators are sensitive to fast neutrons and photons and have excellent pulse shape discrimination (PSD) capabilities. The traditional charge integration (CI) method commonly used for PSD analysis eliminates piled-up pulses and relies on a particle discrimination line to separate neutrons and photons. The presence of the intense photon flux during AI creates a significant number of piled-up events in the stilbene scintillator, thereby posing a great challenge to the traditional CI method. Identifying true single neutron pulses becomes challenging due to the presence of a pile-up cloud and overlapping neutron, photon and pile-up clouds in the PSD analysis. To mitigate the effect of pulse pile-up and identify true single neutron pulses from stilbene scintillators, an artificial neural network (ANN) system is developed. The developed ANN system identifies single neutron pulses and neutron-photon combinations from piled-up events. The results obtained from a ^{252}Cf measurement in the presence of the intense photon flux show that the developed ANN system outperforms the traditional CI method. Since many piled-up events lie above the particle discrimination line, they get misclassified as neutrons by the traditional CI method resulting in 27% overestimation of the net neutron count rate during the linac pulse. The overall net neutron count rate (single and restored neutrons) during the linac pulse, estimated by the ANN system is 62.32% of the ground truth. Energy spectroscopy of the ANN attributed single neutron pulses further provides evidence on the detection of prompt fission neutrons from the ^{252}Cf fission source.

INDEX TERMS Artificial neural network, high photon flux, linac, pile-up recovery, trans-stilbene.

I. INTRODUCTION

Non-destructive assay (NDA) techniques, classified as either passive or active, are widely used to detect radiation emitted from special nuclear materials (SNMs). Passive NDA techniques measure radiation from the spontaneous decay of the nuclear material [1]. In such techniques, the desired signals are the characteristic gamma-ray energies emitted spontaneously as a result of radioactive α or β-particle decay. The shielding around the SNM may cause attenuation of the characteristic gamma rays, thereby limiting passive gamma-ray NDA. Another challenge in passive gamma-ray NDA is the ability of the detector to resolve the different gamma-ray energies. Neutrons that are emitted spontaneously as a result of fission or as a result of (α, n) reaction on low-Z materials are another desired signal in passive NDA. However, not all isotopes of SNM, for example ^{235}U, have high spontaneous fission, thereby limiting neutron emissions. Low neutron emissions limit detection signals and therefore pose a challenge to the passive neutron NDA.

The associate editor coordinating the review of this manuscript and approving it for publication was Xi Peng.

The limitations of passive NDA techniques can be overcome using active NDA. In active NDA, targets of materials are bombarded with an ionizing radiation inducing nuclear reactions that help identify or quantify SNM through fission or isotopic identification [2]. Fission reactions are induced in SNM when irradiated with neutrons or high-energy photons, resulting in emission of 2-3 highly energetic prompt fission neutrons and approximately 8 prompt gamma rays. For up to several minutes after fission, SNM continues to emit delayed neutrons (approximately 0.01–0.02 per fission) and delayed gamma rays (approximately 6-7 per fission) [3]. In active NDA, both prompt and delayed signatures comprise the desired signal. The higher yield from prompt fission signatures has led to the development of many AI systems [4]–[6].

Detection of prompt fission signatures require state-of-the-art detectors, such as the trans-stilbene organic scintillating detector. Unlike the traditional ^{3}He neutron detector that detects thermal neutrons, stilbene can detect fast neutrons. In stilbene organic scintillators, fast neutrons are detected through elastic scatter on hydrogen nuclei whereas gamma rays interact through Compton scatter [7]. The nature of the excited particle determines the fraction of light that appears in the slow component of the scintillator voltage pulse (FIGURE 1a). This dependence allows one to differentiate between particles that deposit the same amount of energy in the detector. The process is referred to as the pulse shape discrimination (PSD) [8] and stilbene organic scintillators have excellent PSD capabilities. A typical PSD plot from a ^{252}Cf spontaneous fission source is shown in FIGURE 1b.

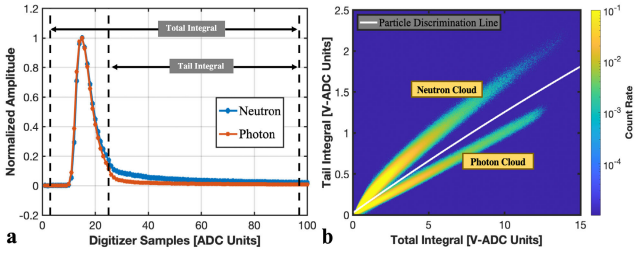

FIGURE 1. a) Traditional charge integration (CI) method for pulse shape discrimination (PSD), and b) An example of PSD contour plot from ^{252}Cf spontaneous fission source (51.41 keVee threshold).

Dual particle sensitivity can present great challenges in environments where one radiation type dominates another, such as in the photon-based AI scenario. In this technique, high energy photons are used to induce photofission reactions in SNM. The intense photon flux during interrogation causes serious pulse pile-up resulting in substantial suppression of the desired neutron signal from photofission. The presence of additional pulses in the pulse tail leads to misclassification of piled-up events as neutrons during PSD.

In this work, an artificial neural network (ANN) system has been developed to mitigate the effect of pulse pile-up in trans-stilbene organic scintillators during photon AI of SNM. The structure of this paper is as follows. A summary of existing literature will provide context on the effectiveness of ANN for nuclear safeguard and non-proliferation applications. We then describe the architecture of the ANN system that has been developed. The following two sections will provide details on the training and testing process of the developed ANN system. We conclude with a discussion on the advantages and disadvantages and thoughts on directly implementing the ANN system on hardware.

II. ARTIFICIAL NEURAL NETWORK IN NUCLEAR SAFEGUARDS AND NON-PROLIFERATION

Artificial intelligence is a technique that enables computers to mimic human behavior. Deep learning is a subset of artificial intelligence that extracts patterns from data using ANNs. The network learns in a similar fashion as the human brain (FIGURE 2). In humans, the learning is at its greatest when they undergo the most dramatic maturational change [9]. With recent technological advances in computing resources, ANN hardware accelerators and deep architectures, such as neural nets (NN), ANN technology has gained maturity to learn complicated functions that can represent high-level abstractions [10]. The detection of SNM is one such high-level abstraction that requires great synchronization of fundamental physics and technology.

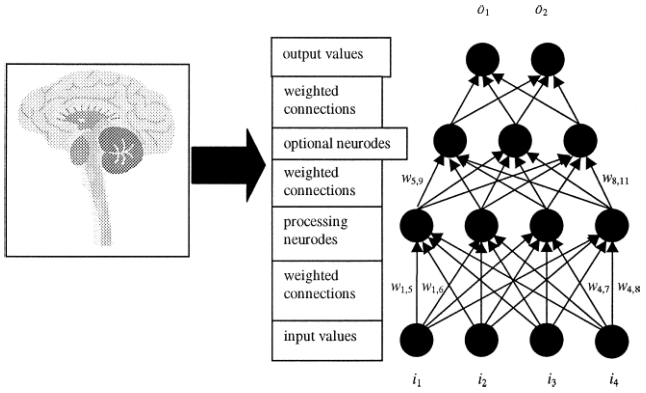

FIGURE 2. Schematic of an artificial neural network inspired from the human brain [11].

As stated earlier, neutrons and gamma rays are the desired signals when trying to detect SNM. Organic scintillators (liquid or solid) are desired in such applications because of their ability to simultaneously detect both radiation types; leading researchers to develop ANN systems for different kinds of organic scintillating detectors. In 2009, Ronchi et. al demonstrated that NN outperforms commonly used two dimensional PSD methods [12]. The detector used by Ronchi et. al was a liquid scintillation detector, BC-501. The authors comment, in the region of small deposited energies, NN provided better classification than conventional PSD methods, is encouraging. The PSD plot represented in FIGURE 1b shows that at low tail and total integral values, the two particle clouds overlap thereby posing a challenge to traditional CI methods. A similar study was performed by Liu et. al in the U.K, where the authors used EJ-301 liquid organic scintillating detector [13]. ANN are also found to have the shortest processing times compared to different PSD methods such as, traditional CI, frequency gradient analysis, K-means++ clustering etc. [14].

Nuclear safeguards require state-of-the-art technology to characterize a nuclear material. NEutron Detector Array (NEDA) is one such state-of-the-art detection system built for multiple applications [15]. NEDA is a versatile device with 331 EJ-301 liquid scintillators that has high detection efficiency, excellent particle discrimination and high-count rate capabilities. Fabian et. al recently developed three different ANN architectures for neutron and gamma ray discrimination in the neutron detector of NEDA [16]. Multi-layer perceptron (MLP), convolutional neural network (CNN) and long short-term memory (LSTM) are the three ANN architectures that were studied by Fabian et. al. The authors concluded that all three ANN architectures performed quite similarly, and LSTM was found to be robust against time misalignment of the scintillator voltage pulse. Another comparative study of ANN architectures was performed in 2013 [17]. Two ANN architectures, namely linear vector quantization (LVQ) and self-organizing maps (SOM), performance was investigated. The investigation found SOM to have superior overall accuracy at all energies.

Piled-up pulses present challenges in PSD analysis. In low-flux scenarios, piled-up pulses are rejected. However, in high radiation environments, such as photon AI, elimination of piled-up pulses can result in huge information loss. If one can decompose individual single pulses from piled-up events, information can be retained. Belli et. al provides a method for recovery of piled-up pulses from NE-213 detector [18]. In this method, the first pulse in a piled-up event is fitted with a response function. The response function is specific to the detector as it is a function of the scintillator's decay constant, and time constant of the measuring circuit. The second pulse is then recovered after subtracting first partially fitted pulse from the piled-up event. The subtraction process continues until all single pulses from the piled-up event are recovered. The process proposed by Belli et. al is non-trivial and quite complex to implement in real time. In 2018, Fu et. al used ANN to recover piled-up pulses [19]. Fu et. al demonstrated the capability of ANN in recovering and identifying neutron and photon composition from piled-up events.

ANN architectures that exist in the literature have demonstrated their potential in nuclear safeguards and nonproliferation applications. Some of the networks even outperformed traditional methods. However, there is very limited literature available for the use of ANN in photon AI scenarios. In this work, the authors aim at developing an economical photon-based AI system using commercially available electron linear accelerator (linac), a trans-stilbene organic scintillating detector and an ANN training platform.

III. DEVELOPED ANN SYSTEM

At the University of Michigan, we developed an ANN system that consists of six NNs. All NNs work in conjunction to produce the desired classification of voltage pulses. The ANN system represented in FIGURE 3 is a unique system in which small well-defined NNs are used to perform detailed classifications. Using multiple NNs allow the flexibility to add classification results in the future without significantly affecting the existing results. Additionally, the ANN system allows for easy interpretation of classification results as well as for updates and future improvements. Our ANN system, in combination with two cleansers, presents a novel approach for classifying single and piled-up pulses from a trans-stilbene organic scintillator.

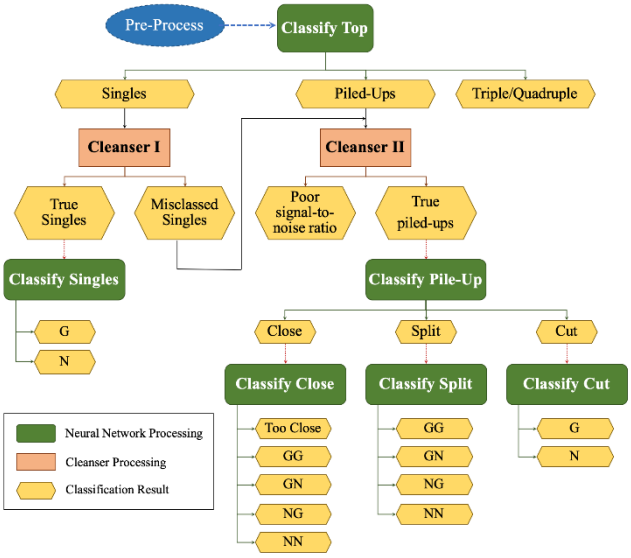

FIGURE 3. ANN system developed for stilbene organic scintillating detector.

Data is pre-processed before it is sent to the ANN system. Pre-processing includes converting ADC units to voltage, flipping the voltage pulse from negative to positive polarity, and performing baseline corrections. The rising edge of each voltage pulse is aligned at 24 ns (12^{th} digitizer sample) using digital constant fraction discrimination (CFD).

After pre-processing the data, Classify Top NN categorizes single, piled-up (double pulses), and triple/quadruple type pulses. The triple/quadruple type pulses are neither recovered nor processed for further classification. Following the singles branch in FIGURE 3, Cleanser I provides an independent verification of the single pulse classification from Classify Top. The independent verification is important because the intense photon flux during AI may introduce additional noise in the voltage pulse that may result in misclassification from Classify Top. If Cleanser I flags pulses as misclass, they are reclassified as piled-up events. If not flagged, these noisy pulses may likely be classified as neutrons by Classify Singles NN because of increased area in the tail. The "true" remaining single pulses are determined to either be a gamma or neutron pulse, represented in FIGURE 3 with a "G" for gamma/photon and an "N" for neutron, in Classify Singles.

Now considering the piled-ups branch of FIGURE 3, Cleanser II processes the piled-up events categorized by Classify Top (and Cleanser I). Cleanser II separates out poor signal-to-noise ratio (SNR) pulses from "true" piled-up events. The "true" piled-up events are then fed into Classify Pile-Up NN to be classified into three groups (close, split, and cut type piled-up events as defined in Section IV). For each

TABLE 1. Structure of neural networks used in the developed ANN system.

NN Processing	Dimension of input layer	Dimension of output layer	Activation function at output layer	Number of hidden layers	Activation function at hidden layers	Dimension of hidden layers
Classify Top*	110	3	Softmax	1	Log sigmoid**	30
Classify Singles*	110	2	Softmax	1	Log sigmoid**	30
Classify Pile-Up	110	3	Softmax	1	Tansig	3
Classify Close*	120	5	Softmax	2	#1: Log sigmoid** #2: Tansig	#1: 30 #2: 10
Classify Split	120	4	Softmax	1	Tansig	7
Classify Cut	120	2	Softmax	1	Tansig	1

* Stacked neural network
** Encoder layer

piled-up category, there is a corresponding NN processing that identifies neutron-photon combinations.

All NNs are fully connected feedforward neural networks that are trained using the scaled conjugate gradient (SCG) learning algorithm [20]. A cross-entropy loss function is implemented to calculate the loss during training of NNs. The maximum number of epochs to train is set to 25,000. The training is terminated when a loss of 1E-3 is achieved on the training dataset. Additionally, if the non-training validation subset loss increases for a consecutive 100 epochs, the network stops training; we call this epoch *n*. At this point, the network disregards the latest 100 epochs and chooses the weights from epoch *n-100*.

The hidden layers in all NNs are aimed to have the smallest dimension to reduce computational complexity while maintaining the performance of the network. The reduced complexity is particularly important for real time FPGA implementation of the ANN in future work. For each NN, we start with an arbitrarily large dimension of the hidden layer. The dimension is gradually reduced, and for each dimension of the hidden layer the NN classification accuracy and error are determined. The percent accuracy and error are obtained from confusion matrices that are generated for each NN from a pre-labelled test dataset. The chosen dimension of the hidden layer is the one at which the percent accuracy is highest and the percent error is the least, except in some cases where the computational complexity cost outweighs the marginal increase in accuracy. TABLE 1 summarizes the structure of NNs used in the ANN system. Following is a more detailed discussion on each NN.

Classify Top is a stacked NN [21] in which an encoder layer is connected to a softmax output layer. A log sigmoid activation function is used for the encoder layer. The dimension of the encoder layer is 30 and the softmax output layer has a dimension of 3. The input vector to the NN consist of 100 Euclidean-normalized samples (1) and 10 segmented maximum values,

$$norm_{(Euclidean)_i} = \frac{S_i}{\sqrt{\sum_{j=1}^{n} S_j^2}} \tag{1}$$

where, S_i is the ith digitizer sample in volts and n is the total number of digitizer samples per voltage pulse. The segmented maximum is found by dividing the Euclidean-normalized voltage pulse, which consist of 100 normalized samples, into 10 segments of 10 samples each. For each segment of 10 samples, the maximum value in the segment is called segmented maximum.

Classify Singles is also a stacked NN in which the encoder layer has a dimension of 30 and the softmax output layer's dimension is 2. Classify Singles NN takes in 100 cumulative distribution function (CDF) samples (3) and 10 segmented maximum values as inputs,

$$norm_{(area)_i} = \frac{S_i}{\sum_{j=1}^{n} S_j} \tag{2}$$

$$CDF_i = \sum_{j=1}^{i} norm_{(area)_j} \tag{3}$$

where, CDF_i is the cumulative distribution function at ith sample. Unlike the Classify Top NN that uses Euclidean-normalized samples for segmented maximum, Classify Singles NN uses 100 area normalized samples (2).

Classify Close NN is a differently stacked NN in which an encoder layer is connected to a hidden layer that is then connected to a softmax output layer. The activation function used for the hidden layer is a hyperbolic tangent sigmoid function (tansig). A log sigmoid activation function is used for the encoder layer that has a dimension of 30. The dimension of tansig hidden layer is 10 and the dimension of softmax output layer is 5. The input vector to the NN consists of 100 Euclidean-normalized samples, 10 segmented maximum values and 10 segmented area values. Segmented area is the area of each segment of the Euclidean-normalized voltage pulse.

Classify Pile-Up, Classify Split and Classify Cut NNs have tansig hidden layer connected to a softmax output layer. All three NNs take in 100 Euclidean-normalized samples and 10 segmented maximum values as inputs. In Classify Split and Classify Cut NNs, 10 segmented area values are also included in the input vector. The dimension of the tansig hidden layer is 3 for Classify Pile-Up NN, 7 for Classify Split NN and 1 for Classify Cut NN. The dimension of softmax output layer is 3 for Classify Pile-Up NN, 4 for Classify Split NN and 2 for Classify Cut NN.

Cleanser I is an autoencoder based cleanser that helps flag pulses with extra noise. The autoencoder consists of two fully connected layers; one is an encoder layer and the other is a

decoder layer. FIGURE 4 provides visualization of the steps performed in Cleanser I. An autoencoder, which is trained on clean single pulses, is used as a denoiser to the original Euclidean-normalized pulse. The decoder from the autoencoder reconstructs the original Euclidean-normalized pulse. There is no noise/ripple present in the reconstructed pulse. The ratio of the absolute difference between reconstructed and original pulse to the reconstructed pulse is computed (4),

$$ratio = \frac{|reconstructed - original|}{reconstructed} \tag{4}$$

where *reconstructed* is the decoded pulse and *original* is the Euclidean-normalized pulse. If the ratio exceeds a set threshold value, the pulse is flagged as a misclassified single pulse. Both the encoder and decoder use a log sigmoid activation function. The encoder layer has a dimension of 30 and the decoder layer's dimension is 100. Cleanser I provides an independent verification to the singles classification produced by the Classify Top NN, thereby increasing confidence in the neutron and photon classification of a single pulse.

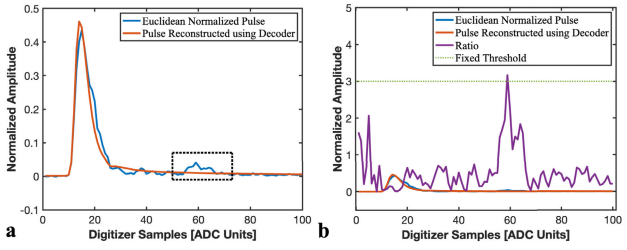

FIGURE 4. a) An example of a noisy pulse decoded using the trained autoencoder, and b) Ratio computed on the noisy pulse.

Cleanser II differentiates poor SNR pulses from "true" piled-up events. The second voltage pulse in the piled-up event must exceed a set threshold for it to be considered as a "true" piled-up event. The threshold is user-specified and all piled-up events that pass the voltage threshold check on the second pulse are sent to the Classify Pile-Up NN for further classification.

IV. TRAINING OF THE DEVELOPED ANN SYSTEM

The ANN system is trained using the Deep Learning Toolbox from MATLAB [22]. Training requires sets of known-neutron and known-photon pulses. A time-of-flight (TOF) measurement is used to collect high-confidence neutron and photon single pulses from a ^{252}Cf spontaneous fission source. To reduce the contribution of gamma rays, start and stop detectors used in the TOF setup are enclosed in 5.08 cm thick lead shielding cave. The measured TOF spectrum is shown in FIGURE 5a. A neutron region is defined in the TOF spectrum. All pulses that belong to the neutron region are subject to PSD using the traditional CI method [23] to remove any present gamma contamination. The traditional CI method and time-tags from the TOF provides high-confidence neutron single pulses. The remaining pulses that lie outside the neutron region are gamma single pulses. A 200 mV (280.8 keVee) threshold is applied to all single pulses for better SNR. FIGURE 5b shows the pulse height distribution

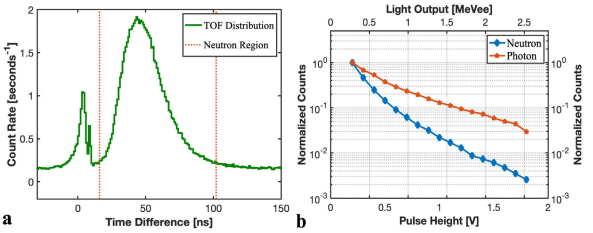

FIGURE 5. a) Measured time-of-flight spectrum from a ^{252}Cf spontaneous fission source, and b) pulse height distribution for the ANN system training data.

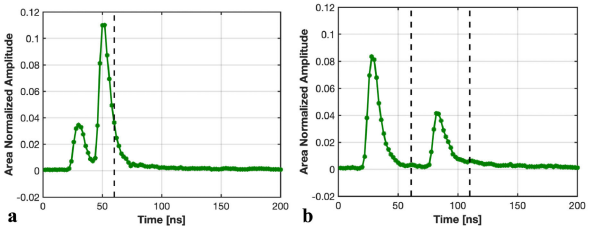

FIGURE 6. A close type piled-up event in which: a) the second voltage pulse is within 60 ns (too-close type), and b) the second voltage pulse is between 60-110 ns.

for the high-confidence neutron and gamma single pulses used for the ANN training.

The clean high-confidence neutron and gamma single pulses are used to synthesize piled-up, triple and quadruple type pulses. The synthesis of piled-up events establishes ground truth training data for the ANN system. Three different kinds of piled-up events; close, split and cut, with definitions based on the time separation between two voltage peaks are synthesized. An example of each type of piled-up event is represented in FIGURE 6 and FIGURE 7. The developed ANN system cannot recover triple, quadruple and too-close type of piled-up events. In the case of cut type piled-up events, only the first voltage pulse is recovered.

The training dataset to the Classify Top NN is 75,000 pulses split evenly between single, close, split, cut and triple/quadruple type pulses. The training of Classify Pile-Up NN is performed using 150,000 pulses comprised of close, split and cut types. Classify Split NN and Classify Cut NN are trained with a total of 80,000 synthesized neutron-photon piled-up events (20,000 piled-up events for a given combination of neutron and photon). The training of Classify Close NN is performed with a total of 75,000 synthesized piled-up events (15,000 pulses for each subtype of close type piled-up events). Classify Singles NN is trained with a total of 30,000 neutron and photon single pulses.

All six NNs are trained individually in a supervised fashion. The three stacked NNs, Classify Top, Classify Singles and Classify Close are trained in three steps. First step includes training of hidden layers in an unsupervised fashion using the autoencoder. This is then followed with the training of the softmax output layer. In the final step, all layers are joined together to form a stacked NN, which is trained for one final time in a supervised fashion.

A small set of the data (5,000 pulses for each single, close, split, cut and triple/quadruple category) is used to test

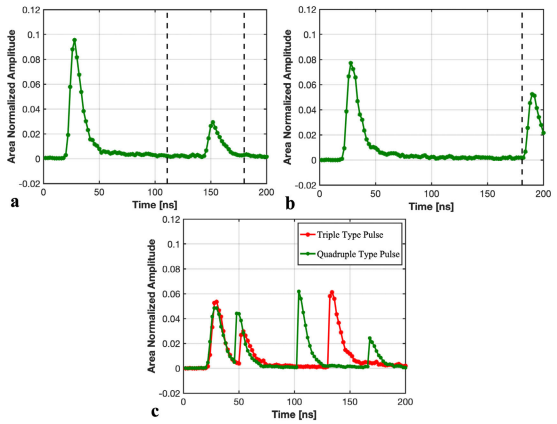

FIGURE 7. a) Split type piled-up event (second voltage peak is between 111-180 ns), b) cut type piled-up event (second voltage peak is past 181 ns), and c) triple/quadruple type pulses.

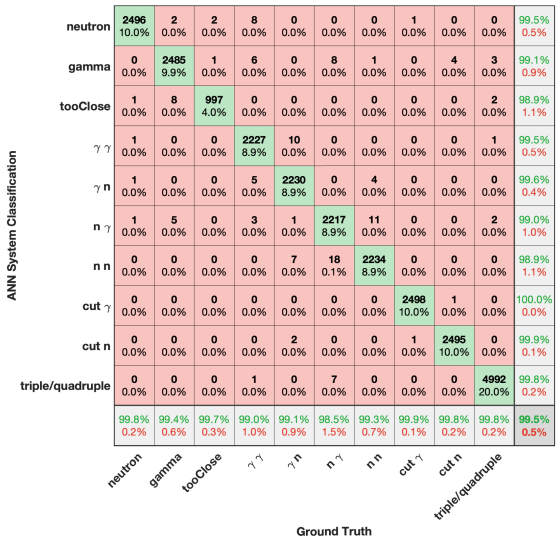

FIGURE 8. Confusion matrix for the developed ANN system.

the performance of the trained ANN system. The confusion matrix generated from the test dataset is given in FIGURE 8. The classification of single pulses produced by the ANN system is 99.60% accurate. The neutron-photon combinations from close and split type piled-up events are identified with an average accuracy of 98.98%. In cut type piled-up events, the classification of the primary voltage pulse is 99.85% accurate. An overall classification accuracy of 99.50% is obtained for the developed ANN system.

V. TESTING ANN SYSTEM IN PRESENCE OF INTENSE PHOTON FLUX

Our laboratory at the University of Michigan houses a 9 MeV endpoint electron linear accelerator (linac) [24] that is very similar to clinical linacs used at hospitals for radiation therapies. Clinical linacs have more practical applications than other accelerators, which are used in laboratories for various experiments. The use of commercially available economical equipment makes the proposed photon-based active interrogation system applicable for infield operations.

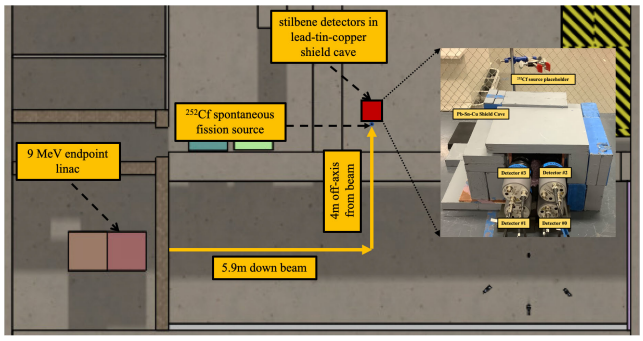

FIGURE 9. Schematic of the experimental setup (top-down view).

The linac produces bremsstrahlung photons that are energetic enough to induce photofission reactions in SNM [25]. ^{252}Cf is a spontaneous fission source that emits prompt fission neutrons; a desired signal during photon AI. We measure a ^{252}Cf neutron source in the presence of the intense bremsstrahlung photon flux from the linac. The ^{252}Cf source is placed off-axis from the linac beam to prevent additional radioactivity being induced as a result of bremsstrahlung bombardment. The measurement of the ^{252}Cf source in the presence of strong photon flux is referred to as the active ^{252}Cf measurement. A passive ^{252}Cf measurement (in the absence of the intense photon flux) establishes ground truth neutron detection rates for the active measurement. The prompt neutron source used in this study is a point source with an activity of 1.21E+03 μCi on the day of the experiment.

We use four trans-stilbene organic scintillating detectors from Inrad Optics [26] coupled to a 51 mm 9214B photomultiplier tube from ET Enterprises [27] to detect prompt fission neutrons. Each detector has a diameter of 5.08 cm and a height of 5.08 cm. The detectors are placed in a lead-tin-copper shield cave to reduce photon flux incident on the detectors. The tin and copper in the shielding cave help shield low energy characteristic Kα and Kβ X-rays that are emitted from lead as a result of high energy bremsstrahlung photon absorption [28]. Data is acquired using CAEN's V1730 16-channel, 14-bit, 500 MS/s digitizer [29]. FIGURE 9 shows the detector setup during active ^{252}Cf measurement.

Active background refers to a background measurement performed in the presence of the intense bremsstrahlung photon flux from the linac and in the absence of a ^{252}Cf neutron source. The laboratory that houses the linac has significant amount of lead and concrete shielding to reduce radiation dose delivered to the public. The 9 MeV bremsstrahlung radiation is energetic enough to induce photonuclear, (g, n), reactions in isotopes of lead and other high-Z targets such as tungsten, copper, etc. [25]. An active background measurement helps to quantify neutrons that are produced through photonuclear reactions in the surrounding laboratory materials.

VI. RESULTS

The linac used for active measurements is a pulsed accelerator that is currently licensed to operate at a repetition rate of 50 Hz. Prompt fission neutrons from hidden SNM will be

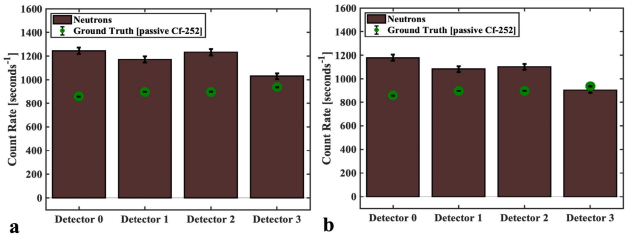

FIGURE 10. Net active ^{252}Cf neutron count rate in all four stilbene organic scintillating detectors determined using the traditional CI method: a) w/o pile-up cleaning, and b) w/ pile-up cleaning (*error bars are from Poisson counting statistics*).

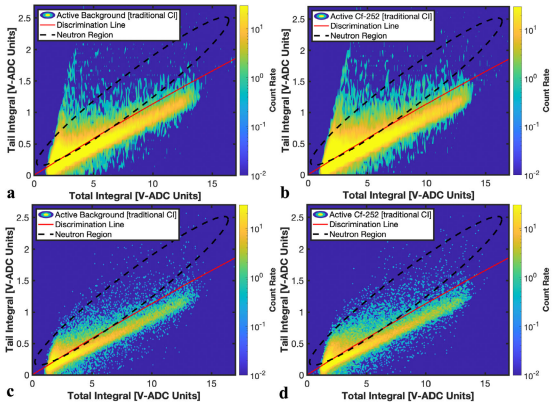

FIGURE 11. Traditional CI PSD contour plots for detector 0: a) active background (w/o pile-up cleaning), b) gross active ^{252}Cf (w/o pile-up cleaning), c) active background (w/ pile-up cleaning), and d) gross active ^{252}Cf (w/ pile-up cleaning). ***Note that the neutron region represented in these plots is for illustration purposes only.***

emitted during the linac pulse. The developed photon-based AI system aims at detecting neutrons during the linac pulse because prompt fission neutrons are more abundant and energetic than delayed neutrons that could be detected between linac pulses. Unlike the linac, the ^{252}Cf spontaneous fission source is a continuous source emitting neutrons at all times. We separate out during-linac-pulse and in-between-linac-pulse voltage signals to identify neutrons that are detected during the bremsstrahlung photon burst from the linac.

A. ACTIVE ^{252}Cf NEUTRON COUNT RATES USING THE TRADITIONAL CI METHOD

During-linac-pulse detections are processed with the traditional CI method [23]. Clipped and below threshold (280.8 keVee threshold) pulses are eliminated in this analysis. Neutrons and photons are separated by a particle discrimination line obtained using an auto slice PSD algorithm [8] on passive ^{252}Cf dataset. Without any pile-up cleaning, net neutron count rates determined by subtracting active background neutron rates from active ^{252}Cf neutron rates exceed ground truth by an average of 38% in detectors 0, 1, and 2 (FIGURE 10a). The overestimation is because of the presence of a pile-up cloud above the particle discrimination line that gets misclassified as neutrons. The overlapping of the neutron, photon, and pile-up clouds (FIGURE 11a and FIGURE 11b) in the PSD plots pose further challenges to particle discrimination and pile-up elimination.

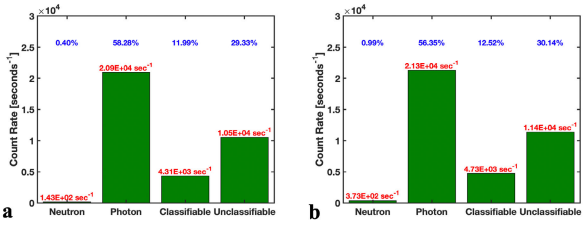

FIGURE 12. ANN system breakdown for detector 0 during: a) active background, and b) active ^{252}Cf.

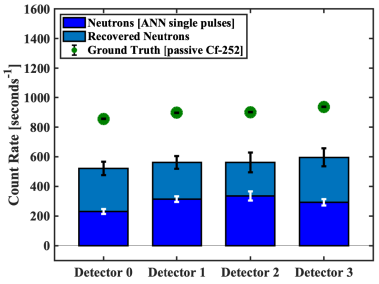

FIGURE 13. Net active ^{252}Cf neutron count rate in all four stilbene organic scintillating detectors determined using the ANN system (*error bars are from Poisson counting statistics*).

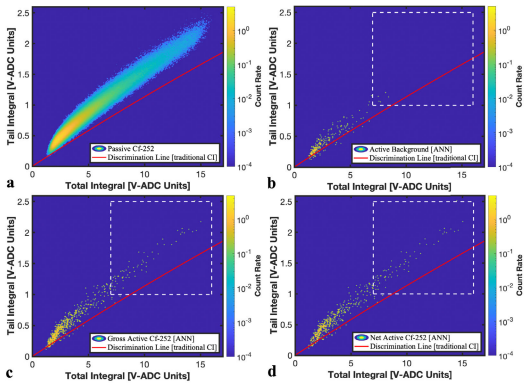

FIGURE 14. Detector 0 PSD contour plots for ANN attributed single neutrons in: a) passive ^{252}Cf, b) active background, c) gross active ^{252}Cf, and d) net active ^{252}Cf.

A fractional pile-up cleaning approach is used to eliminate piled-up events from active measurements. Piled-up events are identified as those having a second voltage pulse with a leading edge that increased by at least 12% of the height of the first voltage pulse in one digitizer step. After pile-up cleaning, there still exists many piled-up events that are misclassified as neutrons (FIGURE 11c and FIGURE 11d) resulting in 27% overestimation of net neutron rates in detector 0, 1 and 2 (FIGURE 10b). A lower fractional cleaning percentage can be used to eliminate remaining piled-up events, however that will result in over-cleaning of the active dataset.

B. ACTIVE ^{252}Cf NEUTRON COUNT RATES USING THE DEVELOPED ANN SYSTEM

For active background and active ^{252}Cf measurements, during-linac-pulse detections are processed with the developed ANN system. FIGURE 12 shows the breakdown of pulses during active background and active ^{252}Cf measurements in detector 0. A significant portion (29%) of the total detected pulses belongs to the unclassifiable category.

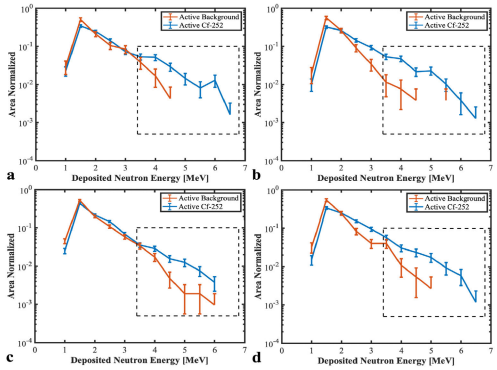

FIGURE 15. Energy spectrum for ANN attributed single neutrons: a) detector 0, b) detector 1, c) detector 2, and d) detector 3.

This unclassifiable category of pulses includes too-close type of piled-up events, triple/quadruple type and poor SNR pulses. Nearly 29% of the total piled-up events (total piled-up events include both classifiable and unclassifiable pulses) are recovered by the ANN system. The other three detectors used during active measurements exhibits similar breakdown of pulses.

FIGURE 13 summarizes overall net neutron count rates as determined by the developed ANN system. Using only single neutron pulses, the net active ^{252}Cf count rates account for an average of 32.55% of the ground truth in all four detectors. When ANN system recovered neutrons are added, the overall net count rate increases to 62.32% of the ground truth. There still exist gaps between the ground truth and the measured net active neutrons due to lost pulses to the unclassifiable category.

The PSD contour plot provides insight on the ANN system classification of single neutron pulses. FIGURE 14 represents a PSD contour plot for the ANN attributed single neutron pulses in detector 0. For reference, passive ^{252}Cf PSD and a particle discrimination line are included. The ANN attributed neutrons from active measurements constitute a neutron cloud in the exact same location as one would expect from passive measurement. The PSD contour verifies the ANN system classification of single neutrons.

Spectroscopic information on the detected neutrons can provide further insight on the ANN system classification. In the case of active background measurement, neutrons are primarily produced through photonuclear reactions on the lead collimator and beamstop in the laboratory. Photoneutrons have limited kinetic energy as determined by the (g, n) reaction Q-value and energy of the interrogating photon. However, fission neutrons can have energies up to 10 MeV or even higher (Watt energy spectrum). The differences in the energy of neutrons that are produced during active interrogation help distinguish high-Z shielding targets from SNMs. Neutron energy spectrum is constructed for ANN attributed single neutron pulses (FIGURE 15). Across all four detectors, active ^{252}Cf has more area than the active background spectrum at higher energies ($>$ 3 MeV). The neutron spectroscopy information obtained from the ANN system provides evidence on the detection of fission neutrons from the ^{252}Cf spontaneous fission source.

VII. CONCLUSION

Detection of hidden SNM is a challenging problem. Constant efforts are being made by researchers across the globe to provide a feasible and economical solution to the problem. In this work, we attempted to provide a solution to SNM detection using active interrogation with commercially available economical equipment. Trans-stilbene organic scintillating detectors are state-of-the-art detectors capable of detecting fast neutrons during the linac pulse. This is the desired signal during photon active interrogation of SNMs.

During photon active interrogation, pulse pile-up is inevitable due to the presence of the intense photon flux. The desired neutron signal is very weak compared to the photon signal. Traditional methods struggle to identify true neutron pulses due to the overlapping neutron, photon and pile-up clouds. The misclassification of piled-up events as neutrons result in overestimation of neutron rates by traditional methods. The ANN system successfully identified single neutron pulses constituting an average of 32.55% of the ground truth neutron rates. Neutron and photon compositions identified from piled-up events helped restore missing information, thereby increasing the overall net neutron rates to 62.32% of the ground truth. Spectroscopic information obtained from the ANN identified single neutron pulses clearly indicates the presence of fission neutrons ($>$3 MeV neutrons) from the ^{252}Cf spontaneous fission source.

In this work, we developed and demonstrated an artificial neural network that can detect prompt fission neutrons with greater accuracy than traditional algorithms during photon active interrogation. The photon active interrogation scenario discussed in this work is used as an example to demonstrate the effectiveness of the proposed detection system. The combined trans-stilbene and artificial neural network system can be used to detect fast neutrons in any high radiation environments. With recent technological advances in ASIC circuits, FPGAs and ANN hardware accelerators, the developed ANN system can be implemented in real time.

REFERENCES

[1] D. Reilly, N. Ensslin, and H. J. Smith, "Passive nondestructive assay of nuclear materials," U.S. Nucl. Regulatory Commission, Washington, DC, USA, Tech. Rep. NUREG/CR-5550, 1991.
[2] R. C. Runkle, D. L. Chichester, and S. J. Thompson, "Rattling nucleons: New developments in active interrogation of special nuclear material," *Nucl. Instrum. Methods Phys. Res. A, Accel. Spectrom. Detect. Assoc. Equip.*, vol. 663, no. 1, pp. 75–95, Jan. 2012.
[3] T. Gozani, "Active nondestructive assay of nuclear materials," U.S. Nucl. Regulatory Commission, Washington, DC, USA, Tech. Rep. NUREG/CR-0602, 1981.
[4] T. F. Grimes, A. R. Hagen, B. C. Archambault, and R. P. Taleyarkhan, "Enhancing the performance of a tensioned metastable fluid detector based active interrogation system for the detection of SNM in <1 m^3 containers using a D–D neutron interrogation source in moderated/reflected geometries," *Nucl. Instrum. Methods Phys. Res. A, Accel. Spectrom. Detect. Assoc. Equip.*, vol. 884, pp. 31–39, Mar. 2018.

[5] S. Van Liew, W. Bertozzi, N. D'Olympia, W. A. Franklin, S. E. Korbly, R. J. Ledoux, and C. M. Wilson, "Identification and imaging of special nuclear materials and contraband using active X-ray interrogation," *Phys. Procedia*, vol. 90, pp. 313–322, Jan. 2017.
[6] C. E. Moss, M. W. Brener, C. L. Hollas, and W. L. Myers, "Portable active interrogation system," *Nucl. Instrum. Methods Phys. Res. Sect. B, Beam Interact. With Mater. At.*, vol. 241, nos. 1–4, pp. 793–797, Dec. 2005.
[7] G. F. Knoll, *Radiation Detection and Measurement*, 4th ed. Hoboken, NJ, USA: Wiley, 2010.
[8] J. K. Polack, M. Flaska, A. Enqvist, C. S. Sosa, C. C. Lawrence, and S. A. Pozzi, "An algorithm for charge-integration, pulse-shape discrimination and estimation of neutron/photon misclassification in organic scintillators," *Nucl. Instrum. Methods Phys. Res. A, Accel. Spectrom. Detect. Assoc. Equip.*, vol. 795, pp. 253–267, Sep. 2015.
[9] J. L. Elman, "Learning and development in neural networks: The importance of starting small," *Cognition*, vol. 48, no. 1, pp. 71–99, Jul. 1993.
[10] Y. Bengio, "Learning deep architectures for AI," *Found. Trends Mach. Learn.*, vol. 2, no. 1, pp. 1–27, 2009.
[11] S. Walczak and N. Cerpa, "A biological basis of artificial neural networks," in *Encyclopedia of Physical Science and Technology*, 3rd ed. New York, NY, USA: Academic, 2001, pp. 631–645.
[12] E. Ronchi, P.-A. Söderström, J. Nyberg, E. A. Sundén, S. Conroy, G. Ericsson, C. Hellesen, M. Gatu Johnson, and M. Weiszflog, "An artificial neural network based neutron–gamma discrimination and pile-up rejection framework for the BC-501 liquid scintillation detector," *Nucl. Instrum. Methods Phys. Res. A, Accel. Spectrom. Detect. Assoc. Equip.*, vol. 610, no. 2, pp. 534–539, Nov. 2009.
[13] G. Liu, M. D. Aspinall, X. Ma, and M. J. Joyce, "An investigation of the digital discrimination of neutrons and γ rays with organic scintillation detectors using an artificial neural network," *Nucl. Instrum. Methods Phys. Res. A, Accel. Spectrom. Detect. Assoc. Equip.*, vol. 607, no. 3, pp. 620–628, Aug. 2009.
[14] T. Ma, H. Song, B. Lyu, and J. Ma, "Comparison of artificial intelligence algorithms and traditional algorithms in detector Neutron/Gamma discrimination," in *Proc. Int. Conf. Artif. Intell. Comput. Eng. (ICAICE)*, Oct. 2020, pp. 173–178.
[15] J. J. Valiente-Dobón, G. Jaworski, A. Goasduff, F. J. Egea, V. Modamio, T. Hüyük, A. Triossi, M. Jastrzab, P. A. Söderström, A. Di Nitto, and G. de Angelis, "NEDA-NEutron detector array," *Nucl. Instrum. Methods Phys. Res. Sect. A Accel. Spectrometers, Detect. Assoc. Equip.*, vol. 927, pp. 81–86, Feb. 2019.
[16] X. Fabian, G. Baulieu, L. Ducroux, O. Stézowski, A. Boujrad, E. Clément, S. Coudert, G. de France, N. Erduran, S. Ertürk, V. González, G. Jaworski, J. Nyberg, D. Ralet, E. Sanchis, and R. Wadsworth, "Artificial neural networks for neutron/γ discrimination in the neutron detectors of NEDA," *Nucl. Instrum. Methods Phys. Res. A, Accel. Spectrom. Detect. Assoc. Equip.*, vol. 986, Jan. 2021, Art. no. 164750.
[17] T. Tambouratzis, D. Chernikova, and I. Pazsit, "A comparison of artificial neural network performance: The case of neutron/gamma pulse shape discrimination," in *Proc. IEEE Symp. Comput. Intell. Secur. Defense Appl. (CISDA)*, Apr. 2013, pp. 88–95.
[18] F. Belli, B. Esposito, D. Marocco, M. Riva, Y. Kaschuck, and G. Bonheure, "A method for digital processing of pile-up events in organic scintillators," *Nucl. Instrum. Methods Phys. Res. A, Accel. Spectrom. Detect. Assoc. Equip.*, vol. 595, no. 2, pp. 512–519, Oct. 2008.
[19] C. Fu, A. Di Fulvio, S. D. Clarke, D. Wentzloff, S. A. Pozzi, and H. S. Kim, "Artificial neural network algorithms for pulse shape discrimination and recovery of piled-up pulses in organic scintillators," *Ann. Nucl. Energy*, vol. 120, pp. 410–421, Oct. 2018.
[20] M. F. Møller, "A scaled conjugate gradient algorithm for fast supervised learning," *Neural Netw.*, vol. 6, no. 4, pp. 525–533, Nov. 1993.
[21] D. Wolpert, "Stacked generalization (stacking)," *Neural Netw.*, vol. 5, no. 2, pp. 241–259, 1992.
[22] *MATLAB and Deep Learning Toolbox Release R2020a*, MathWorks Inc, Natick, MA, USA, 2020.
[23] A. C. Kaplan, M. Flaska, A. Enqvist, J. L. Dolan, and S. A. Pozzi, "EJ-309 pulse shape discrimination performance with a high gamma-ray-to-neutron ratio and low threshold," *Nucl. Instrum. Methods Phys. Res. A, Accel. Spectrom. Detect. Assoc. Equip.*, vol. 729, pp. 463–468, Nov. 2013.
[24] *Linatron M9 & M9A Modular High-Energy X-Ray Source*, VAREX Imaging, Salt Lake City, UT, USA. Accessed: Aug. 31, 2021. [Online]. Available: https://www.varexim aging.com/products/security-industrial/linearaccelerators/linatron-m/linatron-m9
[25] M. Chadwick, M. Herman, P. Obložinský, M. E. Dunn, Y. Danon, A. C. Kahler, D. L. Smith, B. Pritychenko, G. Arbanas, R. Arcilla, and R. Brewer, "ENDF/B-VII.1 nuclear data for science and technology: Cross sections, covariances, fission product yields and decay data," *Nucl. Data Sheets*, vol. 112, no. 12, pp. 2887–2996, 2011.
[26] Inrad Optics. *Scintinel Stilbene Single Crystals*. Accessed: Jul. 8, 2021. [Online]. Available: https://inradoptics.com/pdfs/datasheets/InradOptics_Datasheet_Stilbene_Final.pdf
[27] ET Enterprises. *ET Enterprises 51 mm (2') Photomultiplier 9214B Series Data Sheet*. Accessed: Mar. 27, 2021. [Online]. Available: https://et-enterprises.com/products/photomultipliers/product/p9214b-series
[28] R. D. Deslattes, E. G. Kessler, P. Indelicato, L. de Billy, E. Lindroth, and J. Anton, "X-ray transition energies: New approach to a comprehensive evaluation," *Rev. Modern Phys.*, vol. 75, no. 1, pp. 35–99, Jan. 2003.
[29] CAEN. *CAEN V1730/V1730S 16/8 Channel 14 Bit 500 MS/s Digitizer*. Accessed: Mar. 27, 2021. [Online]. Available: https://www.caen.it/products/v1730/

ABBAS J. JINIA (Member, IEEE) received the M.S. degree in nuclear engineering from Purdue University, in 2018. He is currently pursuing the Ph.D. degree with the Department of Nuclear Engineering and Radiological Sciences, University of Michigan. His research interests include active interrogation techniques for nuclear nonproliferation applications, radiography, neutron die-away techniques, applications of linear accelerators and machine learning techniques for nuclear material detections.

TESSA E. MAURER is currently pursuing the bachelor's degree with the Department of Nuclear Engineering and Radiological Sciences, University of Michigan. Upon completing her degree, she hopes to continue onto the Graduate School in nuclear engineering. Ultimately, she aims to have a career in the public policy sector using a technical background as a base. Her current research interests include machine learning strategies for nonproliferation applications in active interrogation and material detections.

CHRISTOPHER A. MEERT received the B.S.E. degree in nuclear engineering from Purdue University, in 2017. He is currently pursuing the M.S.E. and Ph.D. degrees in nuclear engineering and radiological sciences with the University of Michigan. He has previous experience in commercial nuclear power, radon detection, and tensioned metastable fluid detectors. His current research interests include active interrogation techniques, detection techniques for special nuclear material and contraband, and machine learning algorithms for radiation detection.

MICHAEL Y. HUA (Member, IEEE) received the Ph.D. degree in nuclear engineering and radiological sciences from the University of Michigan. His research interests include radiation detection and measurement theory for criticality safety, nuclear nonproliferation and safeguards, and fusion diagnostics.

S. D. CLARKE (Member, IEEE) received the Ph.D. degree in nuclear engineering from Purdue University, in 2007. He joined the Department of Nuclear and Radiological Sciences, University of Michigan, where he is currently an Associate Research Scientist and the Associate Director of the Consortium for Monitoring, Technology, and Verification. He has more than 15 years of experience performing radiation detection measurements and Monte Carlo modeling. He is the author or coauthor of more than 200 articles in conference proceedings and peer-reviewed journals. His current research interests include active interrogation systems for nuclear nonproliferation, safeguards, and treaty verification applications.

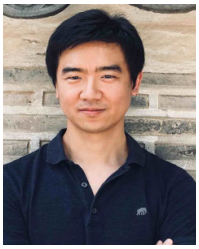

HUN-SEOK KIM (Member, IEEE) received the B.S. degree in electrical engineering from Seoul National University, South Korea, in 2001, and the M.S. and Ph.D. degrees in electrical engineering from the University of California, Los Angeles (UCLA). From 2010 to 2014, he worked as a Technical Staff Member with Texas Instruments. He is currently an Assistant Professor with the University of Michigan, Ann Arbor, MI, USA. His research interests include system analysis, novel algorithms, and efficient VLSI architectures for low-power/high-performance wireless communication, signal processing, computer vision, and machine learning systems. He was a recipient of the 2018 Defense Advanced Research Projects Agency (DARPA) Young Faculty Award (YFA) and the National Science Foundation (NSF) Faculty Early Career Development (CAREER) Award 2019. He is serving as an Associate Editor for IEEE Transactions on Mobile Computing, IEEE Transactions on Green Communications and Networking, and IEEE Solid State Circuits Letters.

DAVID D. WENTZLOFF (Senior Member, IEEE) received the B.S.E. degree in electrical engineering from the University of Michigan, Ann Arbor, MI, USA, in 1999, and the M.S. and Ph.D. degrees from the Massachusetts Institute of Technology, Cambridge, MA, USA, in 2002 and 2007, respectively.

Since August 2007, he has been with the University of Michigan, where he is currently a Professor of electrical engineering and computer science. In 2012, he co-founded PsiKick, a fabless semiconductor company developing ultra-low power wireless SoCs. His research focuses broadly on low-power integrated circuits (ICs) for wireless communication in energy-constrained, such as powered by harvested energy, and volume-constrained, such as cubic-mm sensor nodes applications. More specifically, his research group focuses on: synthesizable all-digital radios and radio building blocks; wireless body sensor networks (channel modeling, radios, and antennas); and radios and interfaces for the mm-scale class of computers. More details can be found at: https://wics.engin.umich.edu. His research interest includes RF integrated circuits, with an emphasis on ultra-low power design. He is a Senior Member of the IEEE Circuits and Systems Society, the IEEE Microwave Theory and Techniques Society, the IEEE Solid-State Circuits Society, and Tau Beta Pi. He was a recipient of the 2009 DARPA Young Faculty Award, the 2009–2010 Eta Kappa Nu Professor of the Year Award, the 2011 DAC/ISSCC Student Design Contest Award, the 2012 IEEE Subthreshold Microelectronics Conference Best Paper Award, the 2012 NSF CAREER Award, the 2014 ISSCC Outstanding Forum Presenter Award, the 2014–2015 Eta Kappa Nu ECE Professor of the Year Award, the 2014–2015 EECS Outstanding Achievement Award, and the 2015 Joel and Ruth Spira Excellence in Teaching Award. He has served on the Technical Program Committee for ICUWB 2008-2010, ISLPED 2011-2015, S3S 2013-2014, RFIC 2013-2021, and ISSCC 2020-2021, and as a Guest Editor for the IEEE Transactions on Microwave Theory and Techniques, *IEEE Communications Magazine*, and the *Journal of Signal Processing: Image Communication* (Elsevier).

SARA A. POZZI (Fellow, IEEE) received the M.S. and Ph.D. degrees in nuclear engineering from the Polytechnic of Milan, Italy, in 1997 and 2001, respectively.

She is currently a Professor of nuclear engineering and radiological sciences and a Professor of physics with the University of Michigan (UM). She is the Founding Director of the Consortium for Verification Technology (CVT) (2014-2019) and the Consortium for Monitoring, Technology, and Verification (MTV) (2019-2024), two large consortia of multiple universities and national laboratories working together to develop new technologies needed for nuclear treaty verification. In this capacity, she directs the work of 25 faculty members and over 250 students engaged in research projects within the consortium. She was named the Inaugural Director of Diversity, Equity, and Inclusion (DEI) with the UM College of Engineering, in 2018. In this capacity, she heads the DEI implementation committee and works to ensure that the students, faculty, and staff are increasingly diverse, everyone is treated equitably, and everyone feels included. Her research interests include the development of new methods for nuclear materials detection, identification, and characterization for nuclear nonproliferation, safeguards, and national security programs.

Dr. Pozzi is a fellow of the American Nuclear Society and the Institute of Nuclear Materials Management. She was a recipient of many awards, including the 2006 Oak Ridge National Laboratory Early Career Award, the 2006 Department of Energy, Office of Science, Outstanding Mentor Award, the 2012 INMM Edway R. Johnson Meritorious Service Award, the 2012 UM Nuclear Engineering and Radiological Sciences Department, Outstanding Achievement Award, the 2017 IEEE Distinguished Lecturer, and the 2018 Rackham Distinguished Graduate Mentoring Award.